The Fifth International Workshop on Micro and Nanotechnology for Power Generation and Energy Conversion Applications
PowerMEMS 2005
Nov. 28-30, 2005
Takeda Hall, The University of Tokyo, Tokyo, Japan

Inherent Orifice Radial Bearing and Hydroinertia Axial Bearing For MEMS-based Turbo Machinery

Yuichi Miura, Piljoong Kang, Shuji Tanaka, Masayoshi Esashi
Tohoku University, 6-6-01 Aza Aoba, Aramaki, Aoba-ku, Sendai, Miyagi

Abstract

This paper describes the design, fabrication and preliminary test of a MEMS-based air turbine with a new gas lubrication system. The gas lubrication system uses a hydroinertia axial bearing to support the rotor from the single side. This configuration is advantageous for optical applications. The radial bearing is a 12-port inherent orifice bearing. To realize this bearing, a new fabrication process called cavity-though DRIE (deep reactive ion etching) has been developed. The fabricated air turbine with a radial bearing gap of 15 μm was tested at various bearing pressures. The maximum rotation speed was 95,000 rpm, which exceeds the estimated critical speeds in the radial, axial and pitching modes.

Keywords: Air bearing, Hydroinertia bearing, Hydrostatic bearing, Turbine, Deep reactive ion etching (DRIE)

1. INTRODUCTION

High speed micro rotating machines are under development for very small gas turbines [1-3], micro turbo pumps [4], polarization modulators [5], polygon mirrors etc. Massachusetts Institute of Technology (MIT) has developed an excellent MEMS-based gas lubrication system for a MEMS-based gas turbine, and achieved a rotation speed of 1.4 million revolution per minute (rpm) [6]. The system adopted an original axial flow hydrostatic air bearing in the radial direction and an narrow gap hydrostatic air bearings in the axial direction.

The MIT's gas lubrication system meets the requirement for their MEMS-based gas turbine, for example, the precise positioning of the impeller for tight tip clearance and small bearing air consumption for small engine efficiency drop. However, the MIT's gas lubrication system must satisfy very tight fabrication tolerances, and seems to have difficulty in yield and robustness for other applications.

We have developed a lubrication system for a MEMS-based air turbine for wide applications including optical devices. For this purpose, it is preferred that one side of the rotor is free from an axial bearing, and that the bearing gaps are wider than that of the MIT's gas lubrication system. A single-sided hydroinertia axial bearing with several tens μm gap has been developed. In this paper, we describe the design, fabrication and first evaluation of the gas lubrication system. Also, hydrostatic inherent gas radial bearing whose bearing orifices are located on the center of the radial bearing hosing was manufactured by special deep reactive ion etching (DRIE) process.

2. DEVICE DESIGN

Overall structure

Figure 1 shows the schematic cross section of the MEMS-based air turbine. This device consists of one through-etched Pyrex glass wafer (first layer) and three silicon wafers (second to fourth layers). The second and third layers are bonded by silicon-to-silicon direct bonding technique, and the first layer and the second-third layer assembly are bonded by anodic bonding technique. The third and fourth layers are bonded by injecting adhesive into alignment/bonding holes formed in each layer.

The first layer (1 mm thick Pyrex glass wafer) is a front cover, and a turbine flow exhaust is installed at the center. A rotor and a radial bearing are fabricated in the second (400 μm silicon wafer) and third (200 μm thick silicon wafer) layers. A hydroinertia axial bearing and a bearing air outlet are installed on the fourth layer (300 μm thick silicon wafer). The bold lines in Fig. 1 show the flow path for the turbine and bearings.

Air turbine

The rotor is 4 mm in diameter and composed of the bonded second and third layers. The radial turbine blades are formed on the front side of the rotor, and the stator vanes are formed on the periphery of the rotor. Figure 2 shows the fabricated rotors and the stator. Pressurized air supplied from the turbine flow inlet port flows radially inward through the rotor blades, and then exhausts axially. The turbine blade shape was designed by velocity triangle method to obtain a rated rotational speed of 300,000 rpm at an air inlet pressure of 440 kPa and a flow rate of 10 slm.

Hydrostatic radial bearing

The radial bearing has 12 bearing orifices with a rectangular opening of 50 μm × 90 μm, as shown in Fig. 3. Each bearing orifice is placed at the center of the 350-μm-long radial bearing housing. This standard configuration is advantageous to supply high-pressure bearing air compared with the axial-flow configuration, because the cross-influence between the radial and axial bearings can be small. This cross-influence problem is critical for the MEMS-based gas lubrication system within the limited area for flow ways and gas ports [3]. The radial bearing pressure plenums around the rotor are divided into 4 parts to control eccentricity. Also, anisotropic pressurization

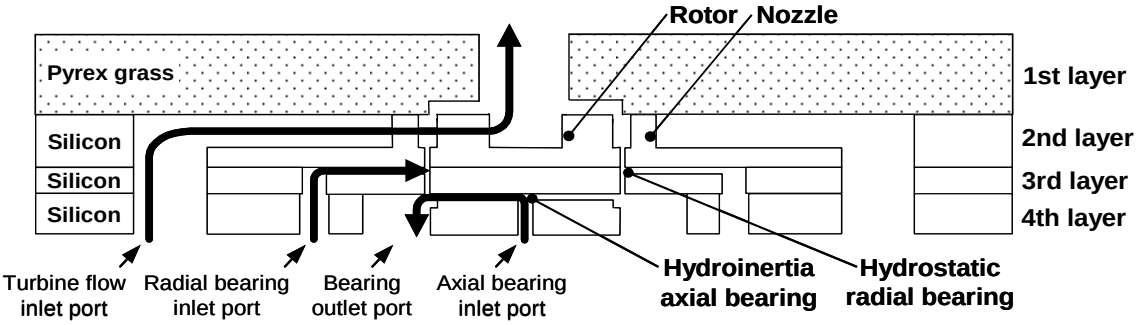

Fig. 1. Cross sectional structure of the air turbine

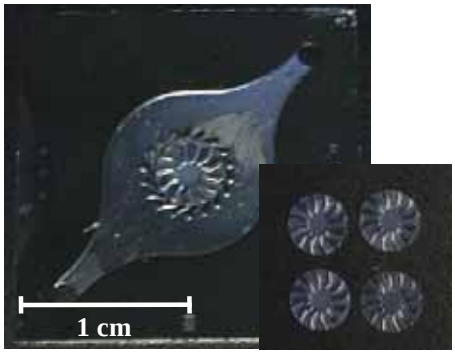

Fig. 2. Fabricated rotors and stator

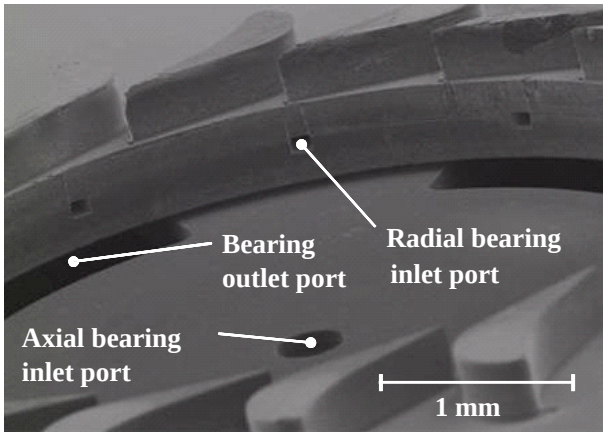

Fig. 3. Gas lubrication system

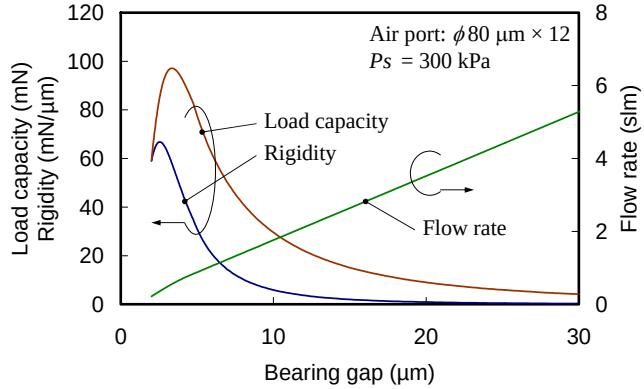

Fig. 4. Design calculation of the hydrostatic radial bearing

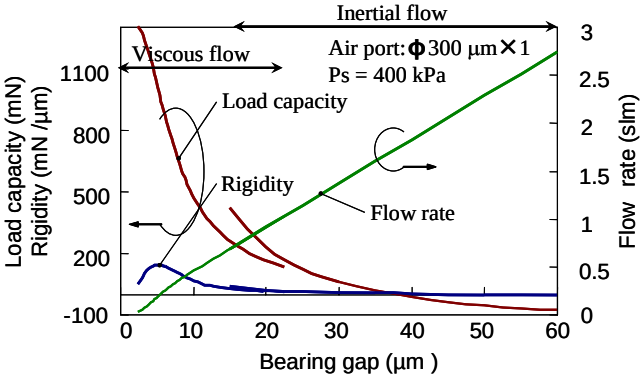

Fig. 5. Design calculation of the hydroinertia axial bearing

is possible to improve whirl stability [7]. At the first test in this study, the 4 radial pressure plenums were evenly pressurized. The calculated load capacity and rigidity of the radial bearing are shown in Fig. 4. The calculation followed the method described in Ref. [8]. The maximum load capacity and rigidity are 100 mN and 60 mN/μm around a bearing clearance of 5 μm, assuming that the orifice diameter is 80 μm, the inlet pressure is 300 kPa, and the eccentricity is 0.5. However, it is not easy to make the bearing gap of 5 μm due to the limit of available DRIE technology. We prepared several rotors with different diameters, and tested a bearing gap of 15 μm in this study.

Hydroinertia axial bearing

The hydroinertia axial bearing is one of externally-pressurized gas bearings, and has several times wider bearing gap than that of a conventional hydrostatic air bearing [9]. The hydroinertia axial bearing which we designed just has a single orifice at the center of the rotor bottom, as shown in Fig. 5. The mechanism of the hydroinertia bearing is explained as follows. When the bearing gap is narrow, air velocity in the bearing gap is below sound speed, and static pressure shows gradually-reducing distribution from the center orifice to the bearing edges. The integral of the static pressure in the bearing gap is positive, and pushes up the rotor. When the bearing gap is sufficiently large, on the other hand, air flow chokes at the exit of the orifice, and radially-expanding air flow becomes supersonic until a shock wave appears as in a

Laval nozzle. The static pressure in the bearing gap monotonously decreases from the center orifice to the shock wave, jumps up at the shock wave, and then reaches the atmospheric pressure at the bearing edge. Thus, the integral of the static pressure in the bearing gap becomes negative on a certain condition to pull back the rotor.

Figure 4 shows the load capacity, rigidity and flow rate of the designed hydroinetia axial bearing. The calculation was done in the inertial (bearing gap: > 15 μm) and viscous (bearing gap: < 22 μm) regions using the method reported in Refs. [8] and [9], respectively. The orifice diameter is assumed to be 300 μm. The calculated load capacity crosses zero at a bearing gap of 38 μm, suggesting that the rotor stably levitates at this bearing gap without axial force. As this calculation shows, the hydroinertia air bearing can support the rotor from the single side. Thus, the upper side of the rotor is easy to be used for applications.

3. FABRICATION

Figure 6 shows the simplified fabrication process of the MEMS-based turbine. All structures in the silicon wafers are fabricated by DRIE. The Pyrex glass top layer is fabricated by wet etching and mechanical drilling. The second and third layers are bonded by direct bonding technique, the first and second layers are bonded by anodic bonding technique, and the third and forth layer are glued.

The key fabrication technology is cavity-through DRIE used at Step 5) in Fig. 6. This special DRIE process has been developed to fabricate the hydrostatic radial bearing with orifices located at the center of the radial bearing housing. The cavity-through DRIE penetrates directly-bonded wafers through cavities formed inside the wafers. In this process, the flow ways and orifices of the radial bearing are fabricated in the third layer at Steps 2) and 3), and then the second layer covers them by direct bonding at Step 4). The cavity-through DRIE at Step 5) makes the radial bearing gap and separates the rotor from the stator, opening the orifices.

The cavity-through DRIE process still has the problem that the side wall becomes partly rough, as shown in Fig. 6. Figures 3 and 7 show different parts in the same sample. The rough side wall appears where the wafers are not bonded. We assume that passivation films deposited in the cavities and bonding interface during Bosch DRIE process disturb etching. Future work to improve the cavity-through DRIE process is necessary to make the as-designed radial bearing.

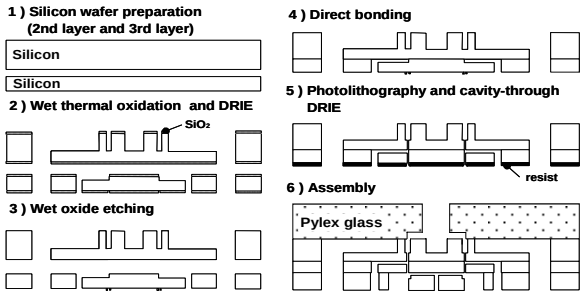

Fig. 6. Fabrication process

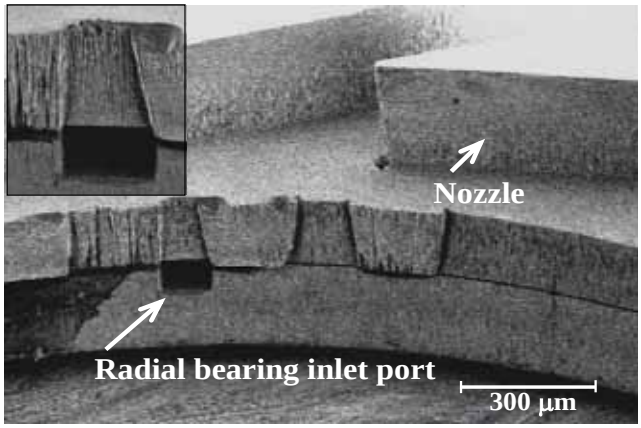

Fig. 7. Rough radial bearing housing fabricated by cavity-through DRIE

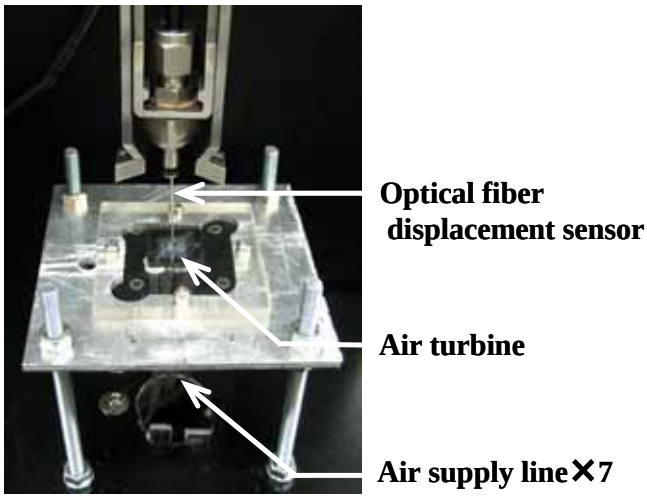

Fig. 8. Setup for the MEMS-based turbine

4. EVALUATION

In this study, the air turbine with the rough surface on the radial bearing housing (Fig. 7) was tested as the first trial. We inserted the rotor which was separately made into the stator as the radial bearing gap became 15 μm. Figure 8 shows an experimental setup. The rotation speed is measured using an optical fiber displacement sensor (Philtec, D-20) by detecting the height of the 12 blades on the rotor. Nylon tubes are used to supply dry air to the bearings and turbine.

We investigated the maximum rotation speed by changing the air supply pressures of the radial and axial bearings. When the axial bearing air was supplied, the rotor was once lifted up and then settled near a height predicted by the calculation (e.g. Fig. 5). After a certain bearing condition was set, the turbine flow rate was increased for acceleration until the rotor stops by bearing crash.

Figure 9 shows the maximum rotation speed and the flow rate of the axial bearing as functions of the axial bearing pressure. The radial bearing pressure was constant at 100 kPa. The maximum rotation speed increased when the axial bearing pressure increased from 300 kPa to 400 kPa, but saturated at 80,000 rpm.

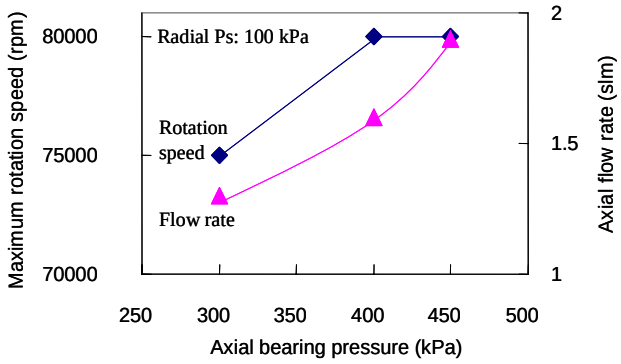

Fig. 9. Maximum rotation speed at different axial bearing pressures

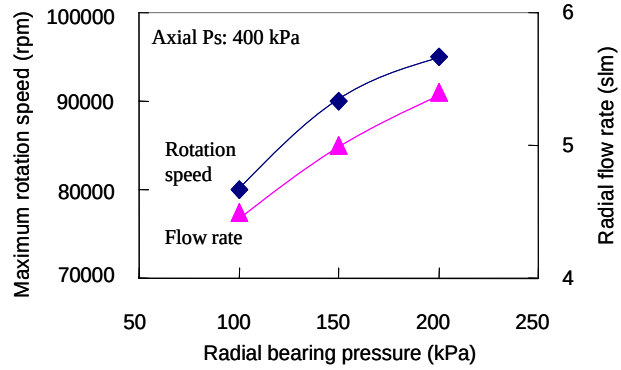

Fig. 10. Maximum rotation speed at different radial bearing pressures

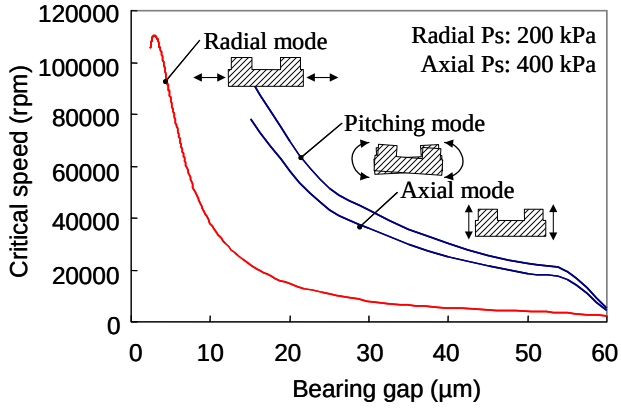

Fig. 11. Estimated critical speeds

Figure 10 shows the maximum rotation speed and the flow rate of the radial bearing as functions of the radial bearing pressure. The axial bearing pressure was constant at 100 kPa. The maximum rotation speed increased with increase in the radial bearing pressure. The maximum rotation speed of 95,000 rpm was obtained at a radial bearing pressure of 200 kPa, but at higher radial bearing pressure, the air turbine did not start up. This could be because the air flow rate was too high for the capacity of the exhaust ports, and the axial bearing did not work normally.

Eventually, the maximum rotation speed was 95,000 rpm in the first test. At this maximum rotation speed, 13 kPa was applied to the turbine inlet. This pressure pushes the rotor down by about 70 mN, and the displacement from the unloaded rotor position is estimated to be about 9 μm. Thus, the axial gap may be about 30 μm at the maximum rotation speed. This suggests that the lack of the axial load capacity is not the reason of the bearing crash.

The resonance of the rotor-bearing system is another possible reason of the bearing crash. Figure 11 shows the estimated critical speeds of the rotor-bearing system assuming that the radial and axial bearing pressures are 200 kPa and 400 kPa, respectively. In this experiment, the radial and axial bearing gap is 15 μm and 30 μm, respectively. Thus, the estimated critical speeds are 22,000 rpm, 36,000 rpm and 43,000 rpm in the radial, axial and pitching modes, respectively. From this estimation, it is thought that the system passed every critical speeds. The critical speeds were estimated using simple spring-mass models, and must be confirmed experimentally in the future.

5. CONCLUSION

A MEMS-based air turbine with a new gas lubrication system was designed, fabricated and preliminarily tested. The gas lubrication system uses a hydroinertia axial bearing to support the rotor from the single side. This configuration is advantageous for optical applications. The radial bearing is a 12-port inherent orifice bearing. To realize this bearing, a new fabrication process called cavity-though DRIE has been developed.

The rotation test was performed using the air turbine with a radial bearing gap of 15 μm. The axial bearing worked as designed. The maximum rotation speed was 95,000 rpm, when the radial and axial bearing pressures are 200 kPa and 400 kPa, respectively. The estimated critical speeds are 22,000 rpm, 36,000 rpm and 43,000 rpm in the radial, axial and pitching modes, respectively. And, the axial gap at the maximum rotational speed is estimated to be about 30 μm. Thus, the limiting factor of the maximum rotation speed is not probably the resonance of the rotor-bearing system or the lack of the axial load capacity.

References

[1] A. H. Epstein *et al.*, "Millimeter-scale, MEMS gas turbine engines", Proc. ASME Turbo Expo 2003, GT-2003-38866.

[2] S. Tanaka *et al.*, "Turbo test rig with hydroinertia air bearings for a palmtop gas turbine", *J. Micromech. Microeng.*, 15, 1449-1454, 2004.

[3] P. Kang *et al.*, "Demonstration of a MEMS-based turbocharger on a single rotor", *J. Micromech. Microeng.*, 15, 1076-1087, 2005.

[4] N. Honda *et al.*, "Micro turbo pump made of low-stress, ultrathick photoresist for portable fuel cell application", Proc. Micro System Technologies, 2005, 48-54.

[5] M. Hara *et al.*, "Rotational infrared polarization modular using a MEMS-based air turbine with different types of journal bearing", *J. Micromech. Microeng.*, 13, 223-228, 2003.

[6] L. G. Fréchette *et al.*, "High-speed microfabricated silicon turbomachinery and fluid film bearings", *J. Microelectromech. Syst.*, 14, 141-152, 2005.

[7] L. X. Liu and Z. S. Spakovszky, "Effects of bearing stiffness anisotropy on hydrostatic micro gas journal bearing dynamic behavior", Proc. ASME Turbo Expo 2005, GT-2005-68199.

[8] S. Togo, Gas bearing design guide book, Kyoritsu Shuppan, 2002 [in Japanese].

[9] H. Hikichi *et al.*, "Hydroinertia gas bearings for micro spinners", *J. Micromech. Microeng.*, 15, S228-S232, 2005.